

A Collision Forecast and Coordination Algorithm in Configuration Control of Missile Autonomous Formation

YONGMING WEN¹, SENTANG WU¹, WENLEI LIU¹, JIA DENG¹,
AND XIONGJUN WU², (Member, IEEE)

¹School of Automation Science and Electrical Engineering, Beihang University, Beijing 100191, China

²802nd Research Institute of Shanghai Academy of Space Flight Technology, The Eighth Academy of China Aerospace Science and Technology Corporation, Shanghai 200090, China

Corresponding author: Y. Wen (wenyongming_buaa@foxmail.com)

The work was supported by the Industrial Technology Development Program under Grant B1120131046.

ABSTRACT In this paper, a formation collision forecast and coordination algorithm (FCFCA) is proposed to avoid collisions in the configuration control of missile autonomous formation (MAF). First, the conditions are derived to forecast collisions of the MAF. Second, the transition target configuration is designed to coordinate collisions. Third, by minimizing the formation group cost, we obtain the optimal transition vector, which can avoid collisions and guarantee the efficiency, safety, and stability of the MAF. Finally, simulation and experiment results are presented to verify the effectiveness of the FCFCA.

INDEX TERMS Collision coordination, collision forecast, formation configuration control, group cost, missile autonomous formation.

I. INTRODUCTION

Missile autonomous formation (MAF) means the missile formation that can autonomously implement missions [1]. The autonomy is mainly reflected in two aspects: (a) MAF can make the formation decisions and guide the formation to implement missions autonomously based on the current task environment information; (b) MAF can guide and hold the formation configuration autonomously according to the current formation configuration commands and avoid collisions throughout the process.

When implementing specific flight missions such as the low-altitude penetration and the saturation attack, in order to maximize the penetration probability, MAF is often required of high dynamic (i.e., the high velocity and the big maneuvering overload), and the flat and dense configuration of MAF. In the situation of limited missile maneuverability, limited quality of network service, limited measurement accuracy of sensors and detectors, and the complex and changeable task environment, the high dynamic, flattening, and densification of MAF increase the probability of collisions among the missile members. It requires the control system of MAF to have good formation configuration control and collision avoidance abilities. It means that the members of MAF can adjust their motion states autonomously, so that the velocity of each member becomes consistent, and the position of each member

is in accordance with the desired relative position relationship on the premise of no collisions. Formation configuration control and collision avoidance are two significant aspects of formation control. In recent decades, many formation control strategies, such as leader–follower [2], virtual leader/virtual structure [3], and behavior based method [4], have been well studied to solve problems of these two aspects.

First and second order sliding-mode controllers were proposed for asymptotically stabilizing the vehicles to a time-varying desired formation and ensured the collision avoidance using a vision system carried by the followers [5]. Park *et al.* [6] proposed a robust adaptive formation controller for electrically driven non-holonomic mobile robots to achieve desired formation tracking and collision avoidance with static and moving obstacles. A leader–follower-based adaptive formation control method was studied for electrically driven non-holonomic mobile robots with limited information to achieve the desired formation and guarantee the collision avoidance [7]. A neural fuzzy formation controller for the formation control of leader-follower multi-agent systems was designed with the capability of online learning and to avoid collisions between neighboring agents [8]. An adaptive proportional integral derivative algorithm was proposed to solve a formation control problem in the leader–follower framework where the leader robot's velocities were unknown

for the follower robots [9]. A novel model predictive control based on receding horizon particle swarm optimization was utilized for formation control of non-holonomic mobile robots by incorporating collision avoidance and control input minimization, and guaranteeing asymptotic stability [10]. The advantages of the leader–follower method are that its control structure is simple, and it is easy to realize. Whereas, the disadvantage is that the formation overall interests are difficult to be guaranteed because the status of leader and the follower is unequal.

A virtual structure adding formation feedback is proposed to achieve a high-precision formation configuration control effect [11]–[13]. Hernandez-Martinez and Bricaire [14] addressed a formation strategy using a virtual leader which had communication with the rest of the follower robots, guaranteeing the convergence to the desired formation, but in principle, which did not avoid inter-agent collisions. A synchronous distributed model predictive control algorithm was proposed to solve the collision avoidance problem of multi-agent systems [15]. The advantage of the virtual leader/virtual structure method is that it is easy to control the formation group behavior based on formation configuration feedback. Whereas, the disadvantage is that the formation configuration is relatively rigid, lack of flexibility and not conducive to collision avoidance.

Tucker Balch *et al.* [4] designed the basic behaviors of the robot and made a comparative study on the 4 basic formation configurations using 3 reference points. The 3-layer (social layer, logic layer, and reaction layer) control system structure based on the behavior was adopted, using social roles to represent the positions of the robots in formation configuration and dynamically allocating positions to the robots to form and hold the formation configuration [16]. A new dual-mode control strategy was proposed: a “safe mode” was defined as an operation in an obstacle-free environment and a “danger mode” was activated when there is a chance of collision or when there were obstacles in the path [17]. A decentralized control strategy was introduced to let a group of robots create a desired geometric formation by means of local interaction with neighboring robots, and the formation shape and the avoidance of collisions between robots were obtained by exploiting the properties of weighted graphs [18]. The advantage of the behavior based method is that it is easy to realize distributed control. Whereas, the disadvantages are that it is difficult to control the formation group behavior and ensure the stability of the formation configuration control.

Besides, there are many novel or integrated formation control strategies proposed. For instance, Dai *et al.* [19] presented four novel collision avoidance processes for non-holonomic mobile robots to generate effective collision-free trajectories when forming and maintaining a formation. A model predictive control approach was proposed for multi-vehicle formation taking into account collision avoidance and velocity limitation with reduced computational burden [20]. Formation control strategies based on position estimation for double-integrator systems were investigated to enable the

agents converge to the formation in a cooperative manner and avoid the inter collision [21].

However, there is some lack of research on the configuration control and collision avoidance for MAF until recently. The control objects in most of literatures are the formations of robots or unmanned aerial vehicles, of which the velocity is relatively slow and the control precision is relatively high compared with those of MAF. In addition, the formation control algorithms in most of literatures are designed based on three flocking rules of Reynolds [22] (namely, cohesion, separation, and alignment). Specifically, the collision avoidance is mostly taken when the real-time distance between two formation members is less than the preset distance. However, as the high dynamic, flat, and dense MAF has relatively low control accuracy and poor navigation precision, most of the above-mentioned formation control algorithms, especially the collision avoidance algorithms, are not suitable to be used directly in MAF. For MAF, when the real-time distance is less than the preset distance, it will bring MAF some shortcomings, such as the big risk of collision, the large fuel consumption, the long transition time, and the “chain effect” (which means the generation of new collisions), which will be analyzed in the following. Furthermore, Most of the literatures did not take the formation overall interests into consideration in the process of collision avoidance, i.e., how to avoid collisions with the smallest group cost is not paid sufficient attention. Whether the above-mentioned problems can be solved reasonably determines whether the final configuration of MAF can be formed and the realization can be fast, safe, and stable.

Consequently, a good formation collision forecast and coordination ability means that MAF can rapidly forecast the formation collisions and coordinate the collisions reasonably by minimizing the group cost of MAF. These are what this paper aims to research.

The main contributions can be summarized as follows. (a) Based on the relative position relationships of each missile and the configuration of MAF, the conditions are derived to forecast collisions of MAF. (b) The transition target configuration is designed to coordinate collisions. We obtain the optimal transition vector by minimizing the formation group cost. (c) The simulation and experiment results validate that the algorithm is able to avoid formation collisions and the “chain effect” of collisions, and shorten the time of formation configuration forming meanwhile ensure the safety and stability of the configuration control of MAF.

The structure of this paper is organized as follows. In Section II, the background and basic knowledge of MAF are presented. Then, the collision of MAF is defined and the problems caused by the traditional formation algorithm are analyzed. In Section III, the formation collision forecast and coordination algorithm (FCFCA) is illustrated in detail, including the collision forecast, the collision coordination and the group cost of MAF. In Section IV, simulation and experiment are conducted to verify the effectiveness of FCFCA. Finally, concluding remarks are given in Section V.

II. PRELIMINARIES

A. BACKGROUND AND BASIC KNOWLEDGE

MAF consists of a set of nodes $v = \{1, 2, \dots, n\}$, where $n \geq 2$ denotes the scale of MAF. Let $q_i \in \mathbb{R}^m$ denote the position of node i (i.e., v_i) for all $i \in v$. The vector $q = \text{col}(q_1, \dots, q_n) \in \mathbb{R}^{mn}$ is called the configuration of MAF. Let $p_i = \dot{q}_i$ denote the velocity of v_i . Let $q_{ij} = q_j - q_i$ denote the position of v_j relative to v_i . Let $p_{ij} = \dot{q}_{ij}$ denote the velocity of v_j relative to v_i . Let $d_{ij} = \|q_{ij}\| = \|q_{ji}\|$ denote the relative distance of v_i and v_j . Let $c_i \in \mathbb{R}^m$ denote the target configuration position of v_i . The vector $c = \text{col}(c_1, \dots, c_n) \in \mathbb{R}^{mn}$ is called the target configuration of MAF. Let $c_{ij} = c_j - c_i$ denote the target configuration position of c_j relative to c_i , where $q_i, p_i, q_{ij}, p_{ij}, c_i, c_{ij} \in \mathbb{R}^m, i, j \in v$. Besides, as the flat configuration of MAF is only allowed to make the collision avoidance maneuvering in the horizontal direction in some cases, the configuration control of the flat MAF is more complicated, but closer to engineering practice than that of MAF in 3D space. Based on the above analysis, the configuration control of the flat MAF in the 2D horizontal plane will be researched in this paper, i.e., $m = 2$.

Lemma (1) Wu [1]: Supposing that the relative safe distance margin $\Delta d_{sij} = d_{ij} - d_{sij}$ of v_i and v_j is ergodic stochastic process, according to the central limit theorem, under the combined effects of various indistinctive random factors, Δd_{sij} approximately obeys the normal distribution with the mathematical expectation of the expected relative safe distance margin $\Delta \mu_{sij} = \mu_{ij} - d_{sij}$, and the variance σ_{ij}^2 , i.e., $\Delta d_{sij} \sim N(\Delta \mu_{sij}, \sigma_{ij}^2)$, where d_{sij} denotes the relative safe distance of v_i and v_j , and μ_{ij} denotes the expected formation distance. Supposing the process of holding relative distance between v_i and v_j is uncorrelated stochastic process, we get

$$\sigma_{ij}^2 = \sigma_i^2 + \sigma_j^2 \tag{1}$$

where σ_i denotes the standard deviation of the relative distance hold by v_i .

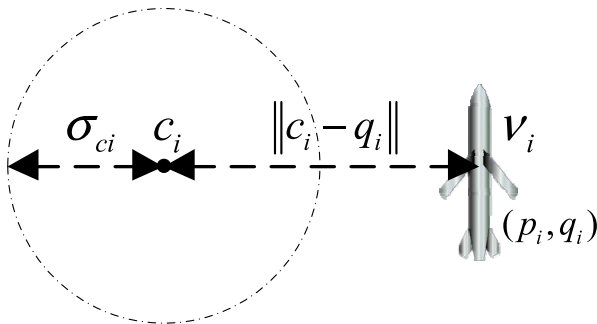


FIGURE 1. Relationship between formation configuration and formation node.

Definition (1): As shown in Fig. 1, the circular region $C_i = \{q_{ci} : \|c_i - q_{ci}\| \leq \sigma_{ci}\}$ with the target configuration position c_i as the center and σ_{ci} as the radius is defined as the configuration circular region, where

$$\sigma_{ci} = k_{ci} \sigma_i \tag{2}$$

and $k_{ci} \geq 0$ denotes the node configuration coefficient of c_i .

Definition (2): The condition under which the formation has formed the target configuration is defined as

$$\|c_i - q_i\| \leq \sigma_{ci}, \quad \forall i \in v. \tag{3}$$

According to (1), (2), and (3), we can get

$$\|c_{ij} - q_{ij}\|^2 \leq \|c_i - q_i\|^2 + \|c_j - q_j\|^2 \leq k_c^2 \sigma_{ij}^2, \quad \forall i, j \in v, i \neq j. \tag{4}$$

Supposing $k_c = k_{c1} = \dots = k_{cn}$, k_c denotes the formation configuration coefficient. The smaller k_c , the more rigid the formation configuration.

According to (4), we can get the condition under which the formation has formed the relative target configuration as follows.

$$\|c_{ij} - q_{ij}\| \leq k_c \sigma_{ij}, \quad \forall i, j \in v, i \neq j. \tag{5}$$

Definition (3): The ‘‘collision’’ in this paper means that the distance between v_i and v_j is less than or equal to the relative safe distance during the formation configuration forming process of MAF (as shown in Fig. 2), namely

$$FC_{ij} : d_{ij} \leq d_{sij}, \quad \|c_{ij} - q_{ij}\| > k_c \sigma_{ij}, \quad \forall i, j \in v, i \neq j \tag{6}$$

where the collision is denoted by FC_{ij} .

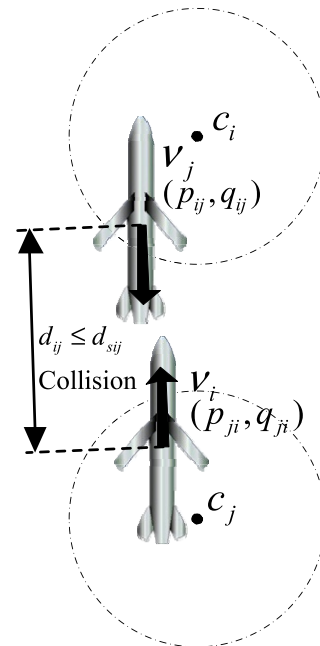


FIGURE 2. Collision of MAF.

It should be noted that the ‘‘collision’’ in this paper means the potential risk of collision, instead of meaning $d_{ij} = 0$.

B. ASSUMPTIONS

1) The members of MAF can obtain the information of local absolute positions and velocities through the navigation system in real time.

2) The communication network of MAF is fully-connected through the one hop or multi-hop pattern.

C. PROBLEM DESCRIPTION

As shown in Fig. 2, since the relative target configuration position c_{ij} is approximately opposite to the relative position q_{ij} , the distance d_{ij} will be quickly reduced by the formation configuration control algorithm. When $d_{ij} \leq d_{sij}$, d_{ij} will increase because of the collision avoidance algorithm based on three flocking rules of Reynolds. Afterwards, the process will be repeated until their lateral distance is greater than d_{sij} . For the high dynamic, flat, and dense MAF studied in this paper, the shortcomings of the traditional collision avoidance algorithm are as follows. (a) d_{ij} fluctuates around d_{sij} for a long time, and due to the large inertia and low control precision of high dynamic MAF, the probability of collision among the members will increase. (b) The continuous accelerating and decelerating maneuvering of v_i and v_j not only consume a large amount of fuel, but also have a high demand of performance of the engine. (c) The forming process of the lateral distance between v_i and v_j requires a long time, which causes that the forming process of the formation configuration is slow. (d) The ‘‘chain effect’’ of MAF means that the dynamic behavior of any node will cause the joint effect of the collision avoidance maneuver of neighbor nodes, and the disturbance caused by the joint collision avoidance will transfer gradually. During the process of collision avoidance between v_i and v_j , the ‘‘chain effect’’ is prone to occurring. In summary, these shortcomings are not beneficial to the safety, stability and efficiency of MAF.

III. FORMATION COLLISION FORECAST AND COORDINATION ALGORITHM

A. COLLISION FORECAST

Theorem (1): The necessary and sufficient conditions under which the potential collision exists between v_i and v_j are

$$\left\{ \begin{array}{l} \text{(a): } \|c_{ij} - q_{ij}\| > k_c \sigma_{ij} \\ \text{(b): } \frac{c_{ij} \cdot (c_{ij} - q_{ij})}{\|c_{ij} - q_{ij}\|} > k_c \sigma_{ij} \\ \text{(c): } \frac{c_{ij} \cdot q_{ij}}{\|q_{ij}\|^2} < 1 \\ \text{(d): } \|c_{ij}\|^2 - \frac{[c_{ij} \cdot (c_{ij} - q_{ij})]^2}{\|c_{ij} - q_{ij}\|^2} \leq d_{sij}^2 \end{array} \right. \quad (7)$$

The physics meaning of (7)-(a) is that q_{ij} has not formed c_{ij} yet. The physics meaning of (7)-(d) is that the minimum of d_{ij} is less than or equal to d_{sij} , where (7)-(b) and (c) are the conditions under which the minimum of d_{ij} is the expression on the left of the inequality (7)-(d).

Proof: According to *Definition (3)*, the necessary and sufficient condition under which the potential collision exists

between v_i and v_j is that when $\|c_{ij} - q_{ij}\| > k_c \sigma_{ij}$, $\exists d_{ij} < d_{sij}$, i.e., $d_{ij \min} < d_{sij}$.

Let $\widehat{d}_{ij}(k)$, $\Delta \widehat{d}_{ij}(k)$ and $\widehat{q}_{ij}(k)$ respectively denote the predicted values of d_{ij} , $\|c_{ij} - q_{ij}\|$ and q_{ij} , namely

$$\begin{cases} \widehat{d}_{ij}(k) = \|\widehat{q}_{ij}(k)\| \\ \Delta \widehat{d}_{ij}(k) = \|c_{ij} - \widehat{q}_{ij}(k)\| \end{cases} \quad (8)$$

where $k \in \mathbb{N}$ denotes the number of prediction. Since the predicted deviation ($c_{ij} - \widehat{q}_{ij}(k)$) is the main factor to generate predicted relative velocity $\widehat{p}_{ij}(k)$, their relationship can be approximated as

$$\begin{cases} \widehat{p}_{ij}(k) = k_{qp} \cdot (c_{ij} - \widehat{q}_{ij}(k)) \\ \widehat{q}_{ij}(k+1) = \widehat{q}_{ij}(k) + \widehat{p}_{ij}(k) \cdot t_c \end{cases} \quad (9)$$

where k_{qp} denotes the proportionality coefficient and t_c denotes the step of prediction. Through iterating (9), we can get

$$c_{ij} - \widehat{q}_{ij}(k) = (1 - t_c \cdot k_{qp})^k (c_{ij} - \widehat{q}_{ij}(0)). \quad (10)$$

The condition of convergence of (10) is

$$|1 - t_c \cdot k_{qp}| < 1 \Rightarrow \lim_{k \rightarrow +\infty} (\|c_{ij} - \widehat{q}_{ij}(k)\|) = 0. \quad (11)$$

Let (10) be expressed as a continuous function. Then modulus operation is performed on both sides of the equation, we can get

$$\begin{aligned} \Delta \widehat{d}_{ij}(t) &= \|c_{ij} - \widehat{q}_{ij}(t)\| \\ &= (1 - t_c \cdot k_{qp})^t \|c_{ij} - \widehat{q}_{ij}(t_0)\| = m^t \Delta \widehat{d}_{ij}(t_0) \end{aligned} \quad (12)$$

where t_0 denotes the predicted start time and

$$m = 1 - t_c \cdot k_{qp}, \quad 0 < m < 1. \quad (13)$$

According to (12), it is easily known that $\Delta \widehat{d}_{ij}(t)$ is a monotonically decreasing function. Since $\Delta \widehat{d}_{ij}(t)_{\min} = k_c \sigma_{ij}$, the range of m^t can be derived as follows:

$$m^t \in \left[\frac{k_c \sigma_{ij}}{\Delta \widehat{d}_{ij}(t_0)}, 1 \right] = \left[\frac{k_c \sigma_{ij}}{\|c_{ij} - \widehat{q}_{ij}(t_0)\|}, 1 \right] \quad (14)$$

Let (10) be expressed as a continuous function, then

$$\widehat{d}_{ij}(t) = \|\widehat{q}_{ij}(t)\| = \|c_{ij} - m^t (c_{ij} - \widehat{q}_{ij}(t_0))\|. \quad (15)$$

The condition under which the potential collision exists between v_i and v_j can be expressed as

$$\widehat{d}_{ij}(t)_{\min} \leq d_{sij}, \quad m^t \in \left[\frac{k_c \sigma_{ij}}{\|c_{ij} - \widehat{q}_{ij}(t_0)\|}, 1 \right] \quad (16)$$

Square on both sides of (15), and take the derivative of t . We can get

$$\begin{aligned} \frac{d(\widehat{d}_{ij}^2(t))}{dt} &= -2m^t \ln(m) (c_{ij} - \widehat{q}_{ij}(t_0)) \\ &\quad \cdot [c_{ij} - m^t (c_{ij} - \widehat{q}_{ij}(t_0))]. \end{aligned} \quad (17)$$

Set (17) equal to 0, then we can get

$$m^{t_s} = \frac{c_{ij} \cdot (c_{ij} - \widehat{q}_{ij}(t_0))}{\|c_{ij} - \widehat{q}_{ij}(t_0)\|^2} \quad (18)$$

where t_s is the moment to obtain the extremum. The minimum value of $\widehat{d}_{ij}(t)$ is discussed in 3 different cases below.

Condition (I): When $m^{t_s} \leq \frac{k_c \sigma_{ij}}{\|c_{ij} - \widehat{q}_{ij}(t_0)\|}$, i.e., $\frac{c_{ij} \cdot (c_{ij} - \widehat{q}_{ij}(t_0))}{\|c_{ij} - \widehat{q}_{ij}(t_0)\|} \leq k_c \sigma_{ij}$, by substituting it into (15), we can get

$$\begin{aligned} \widehat{d}_{ij}(t)_{\min} &= \widehat{d}_{ij}(\log_m^{\left(\frac{k_c \sigma_{ij}}{\|c_{ij} - \widehat{q}_{ij}(t_0)\|}\right)}) \\ &= \left\| c_{ij} - \frac{k_c \sigma_{ij}}{\|c_{ij} - \widehat{q}_{ij}(t_0)\|} (c_{ij} - \widehat{q}_{ij}(t_0)) \right\|. \end{aligned} \quad (19)$$

Therefore, on this occasion, the condition under which the potential collision exists between v_i and v_j is

$$\left\| c_{ij} - \frac{k_c \sigma_{ij}}{\|c_{ij} - \widehat{q}_{ij}(t_0)\|} (c_{ij} - \widehat{q}_{ij}(t_0)) \right\| \leq d_{sij}. \quad (20)$$

Let t_f denotes the time when $q_{ij}(t)$ has formed c_{ij} . According to (15), it is easily obtained that the range of $d_{ij}(t_f)$ is contained in $[\mu_{ij} - k_c \sigma_{ij}, \mu_{ij} + k_c \sigma_{ij}]$. In order to guarantee the safety of MAF, $\mu_{ij} - k_c \sigma_{ij} > \widehat{d}_{sij}$ must be satisfied in the design phase. Therefore we can derive $d_{ij}(t_f) > d_{sij}$. However, the situation described in *Condition (I)* denotes that when q_{ij} has formed c_{ij} , $d_{ij}(t_f) \leq \widehat{d}_{sij}$, which will not occur in engineering practice. Therefore, *Condition (I)* is generally not satisfied.

Condition (II): When $m^{t_s} \geq 1$, i.e., $\frac{c_{ij} \cdot \widehat{q}_{ij}(t_0)}{\|\widehat{q}_{ij}(t_0)\|^2} \geq 1$, by substituting it into (15), we can get

$$\widehat{d}_{ij}(t)_{\min} = \widehat{d}_{ij}(\log_m^1) = \|\widehat{q}_{ij}(t_0)\|. \quad (21)$$

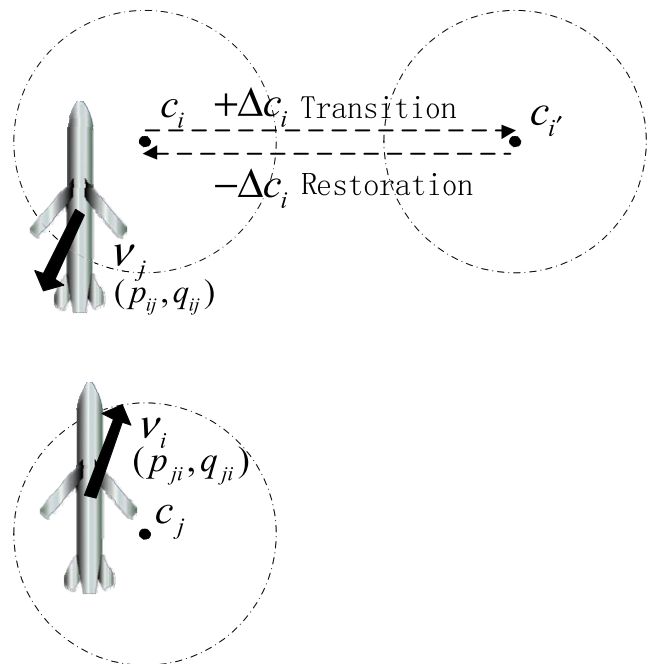


FIGURE 3. Moving collision configuration positions.

Therefore, on this occasion, the condition under which the potential collision exists between v_i and v_j is

$$\|\widehat{q}_{ij}(t_0)\| \leq d_{sij}. \quad (22)$$

Because of the introduction of FCFCA, $d_{ij} > d_{sij}$ will be guaranteed in the configuration control of MAF. However, the situation described in *Condition (II)* denotes that $d_{ij} \leq d_{sij}$, which will not occur in engineering practice as well. Therefore, *Condition (II)* is also generally not satisfied.

Condition (III): When $\frac{k_c \sigma_{ij}}{\|c_{ij} - \widehat{q}_{ij}(t_0)\|} < m^{t_s} < 1$, i.e., $\frac{c_{ij} \cdot (c_{ij} - \widehat{q}_{ij}(t_0))}{\|c_{ij} - \widehat{q}_{ij}(t_0)\|} > k_c \sigma_{ij}$ and $\frac{c_{ij} \cdot \widehat{q}_{ij}(t_0)}{\|\widehat{q}_{ij}(t_0)\|^2} < 1$, by substituting (18) into (15), we can get

$$\begin{aligned} \widehat{d}_{ij}(t)_{\min} &= \widehat{d}_{ij} \left(\log_m^{\left(\frac{c_{ij} \cdot (c_{ij} - \widehat{q}_{ij}(t_0))}{\|c_{ij} - \widehat{q}_{ij}(t_0)\|^2} \right)} \right) \\ &= \left\| c_{ij} - \frac{c_{ij} \cdot (c_{ij} - \widehat{q}_{ij}(t_0))}{\|c_{ij} - \widehat{q}_{ij}(t_0)\|^2} (c_{ij} - \widehat{q}_{ij}(t_0)) \right\|. \end{aligned} \quad (23)$$

Therefore, on this occasion, the condition under which the potential collision exists between v_i and v_j is

$$\left\| c_{ij} - \frac{c_{ij} \cdot (c_{ij} - \widehat{q}_{ij}(t_0))}{\|c_{ij} - \widehat{q}_{ij}(t_0)\|^2} (c_{ij} - \widehat{q}_{ij}(t_0)) \right\| \leq d_{sij}. \quad (24)$$

Simplify (24), then we can get

$$\|c_{ij}\|^2 - \frac{[c_{ij} \cdot (c_{ij} - \widehat{q}_{ij}(t_0))]^2}{\|c_{ij} - \widehat{q}_{ij}(t_0)\|^2} \leq d_{sij}^2. \quad (25)$$

TABLE 1. Initial state of MAF at t=500.0s.

Initial position/m	Configuration position/m
$q_1 = (3816.6, 0.1)^T$	$c_1 = (0.0, 0.0)^T$
$q_2 = (2812.3, 1000.0)^T$	c_2 from $(-1000.0, 1000.0)^T$ to $(0.0, 1000.0)^T$
$q_3 = (3823.5, 2000.0)^T$	$c_3 = (0.0, 2000.0)^T$
$q_4 = (2810.1, 0.0)^T$	$c_4 = (-1000.0, 0.0)^T$
$q_5 = (3811.7, 1000.1)^T$	c_5 from $(0.0, 1000.0)^T$ to $(-1000.0, 1000.0)^T$
$q_6 = (2824.0, 2000.1)^T$	$c_6 = (-1000.0, 2000.0)^T$



FIGURE 4. Initial state of MAF at t = 500.0s.

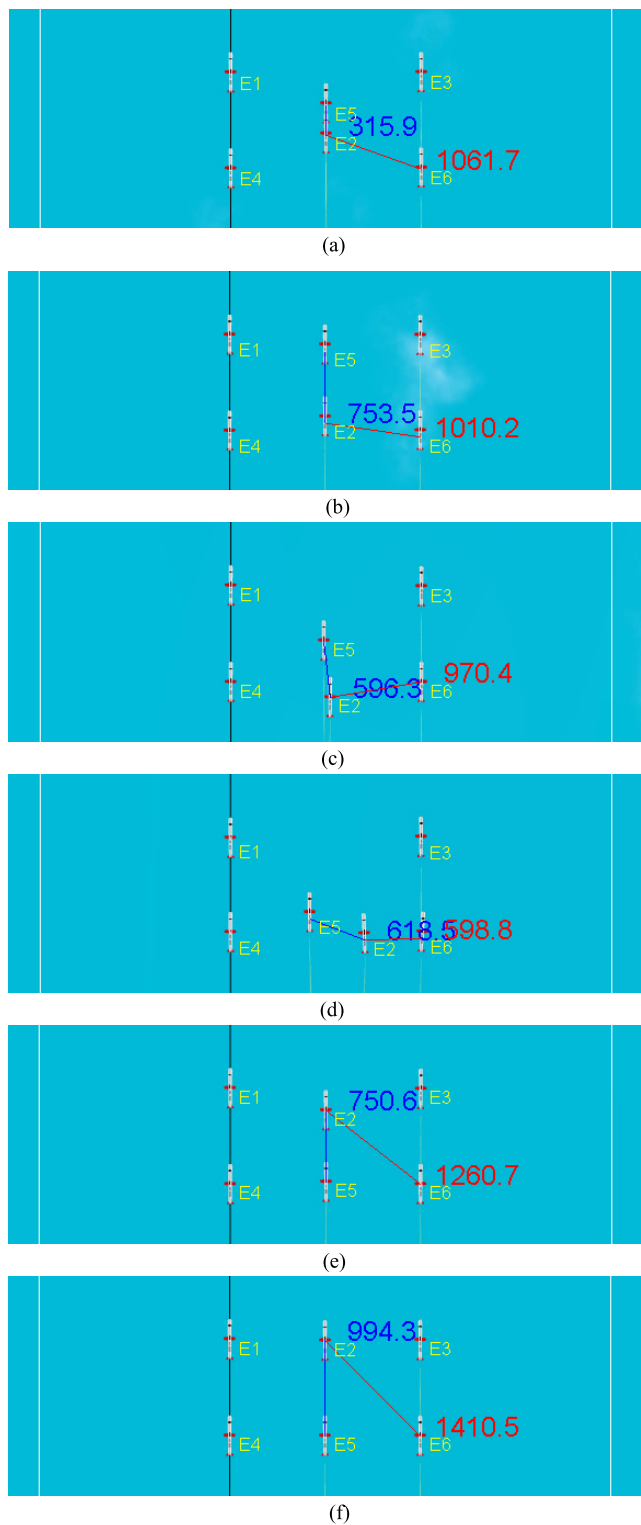


FIGURE 5. Formation configuration control process without FCFA. (a) $t = 520.4s$. (b) $t = 536.7s$. (c) $t = 650.2s$. (d) $t = 676.2s$. (e) $t = 711.1s$. (f) $t = 800.1s$.

Only *Condition (III)* may appear in the engineering practice, so whether c_{ij} and q_{ij} can satisfy *Condition (III)* is the only condition required to be verified to forecast the potential collision between v_i and v_j .

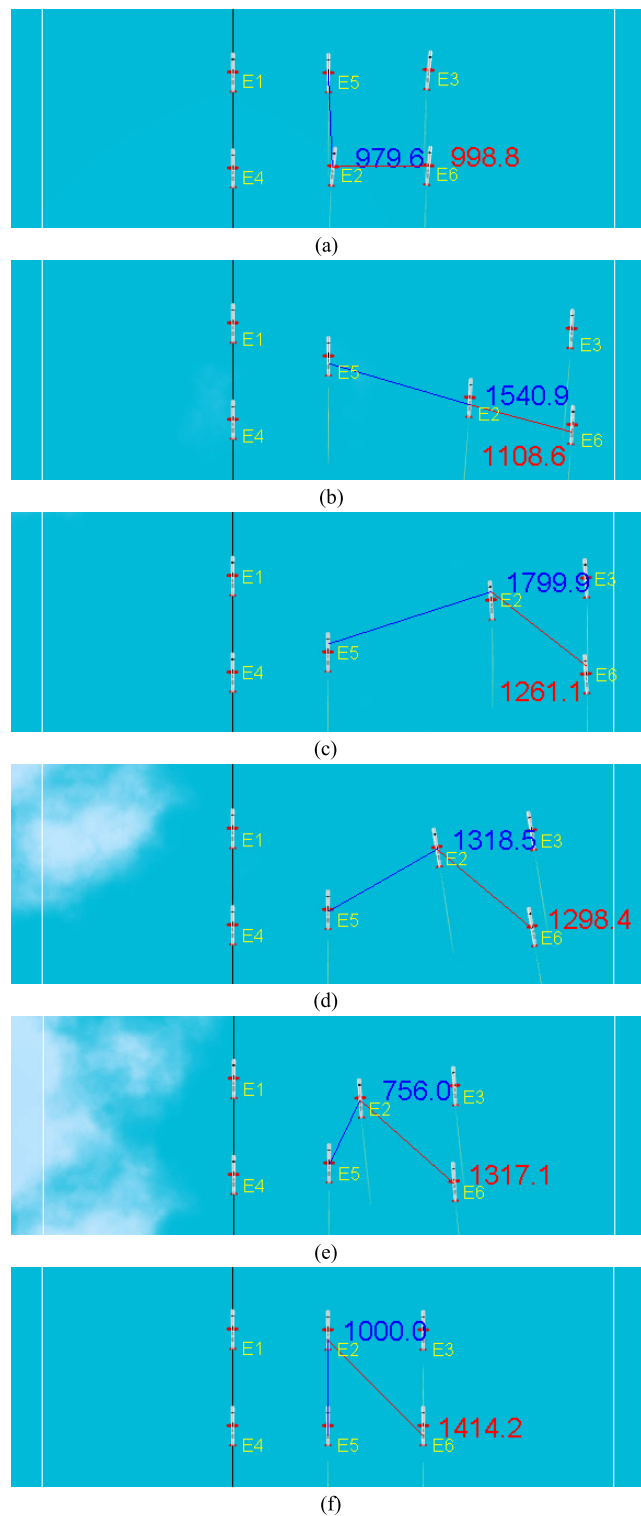


FIGURE 6. Formation configuration control process with FCFA. (a) $t = 502.6s$. (b) $t = 516.4s$. (c) $t = 543.9s$. (d) $t = 549.9s$. (e) $t = 556.7s$. (f) $t = 733.8s$.

B. COLLISION COORDINATION

In order to coordinate the collision FC_{ij} , a transition target configuration denoted by $c_{ij} = c_j - c_i$ is designed, where $c_i = c_i + \Delta c_i$ denotes the transition target configuration

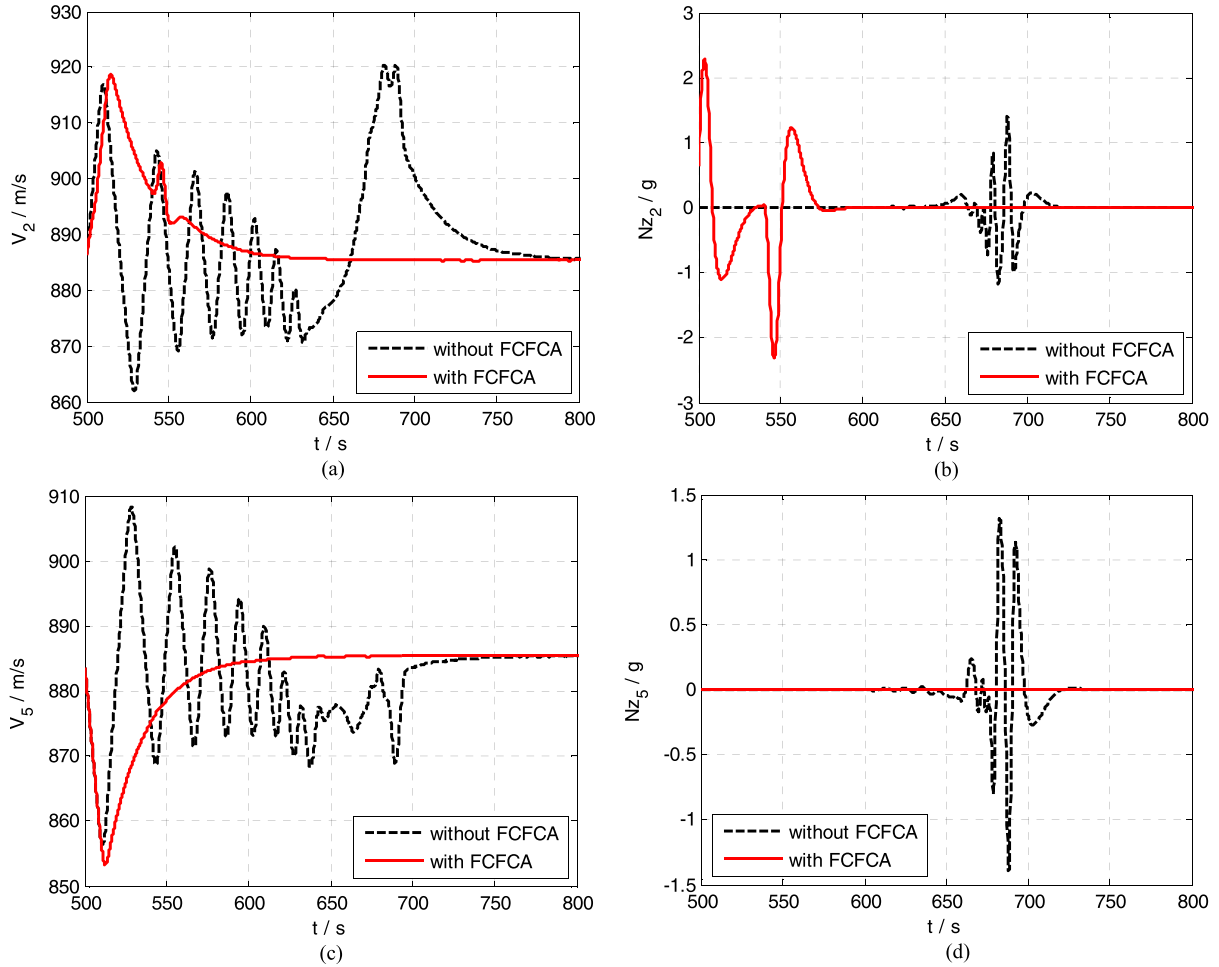


FIGURE 7. Dynamic characteristics of v_2 and v_5 . (a) Velocity of v_2 . (b) Lateral overload of v_2 . (c) Velocity of v_5 . (d) Lateral overload of v_5 .

position of v_i and $\Delta c_i \in \mathbb{R}^2$ denotes the transition vector. When $\|c_{ij} - q_{ij}\| \leq k_c \sigma_{ij}$, c_{ij} should be restored to c_{ij} , so that q_{ij} can form the final target configuration c_{ij} (as shown in Fig. 3).

The transition vector Δc_i should be designed to guarantee that there is no collision during the process of transition and restoration. The constraints of Δc_i or c_{ij} are shown in (26).

$$\left\{ \begin{array}{l} (a) : \|c_{ij} - q_{ij}\| > k_c \sigma_{ij}, \quad \frac{c_{ij} \cdot (c_{ij} - q_{ij})}{\|c_{ij} - q_{ij}\|} > k_c \sigma_{ij}, \\ \frac{c_{ij} \cdot q_{ij}}{\|q_{ij}\|^2} < 1, \quad \|c_{ij}\|^2 - \frac{[c_{ij} \cdot (c_{ij} - q_{ij})]^2}{\|c_{ij} - q_{ij}\|^2} > d_{sij}^2 \\ (b) : \|c_{ij} - c_{ij}\| > k_c \sigma_{ij}, \quad \frac{c_{ij} \cdot (c_{ij} - c_{ij})}{\|c_{ij} - c_{ij}\|} > k_c \sigma_{ij}, \\ \frac{c_{ij} \cdot c_{ij}}{\|c_{ij}\|^2} < 1, \quad \|c_{ij}\|^2 - \frac{[c_{ij} \cdot (c_{ij} - c_{ij})]^2}{\|c_{ij} - c_{ij}\|^2} > d_{sij}^2 \end{array} \right. \quad (26)$$

where (26)-(a) and (26)-(b) denote the conditions under which no collision between v_i and v_j exists during the process of transition and restoration respectively.

If v_i collides with other nodes $v_k (k \in \nu, k \neq i, j)$ during the collision coordination of FC_{ij} , i.e., q_{ki} and c_{ki} meet (7), c_{ki} or Δc_k should be designed according to the above constraints like (26). Therefore, some reasonable transition vectors $\Delta c_i (i \in \nu)$ should be designed to coordinate the collisions one by one. At the same time, the ‘‘chain effect’’ which means the generation of new collisions will be avoided as well.

C. GROUP COST

The group cost of MAF g_f is designed to get the reasonable transition vectors.

$$g_f = g_t + g_r \quad (27)$$

where

$$g_t = \|c_{ij} - q_{ij}\| \quad (28)$$

denotes the transition cost, and

$$g_r = \|c_{ij} - c_{ij}\| \quad (29)$$

denotes the restoration cost.

Thus, the design of transition vectors Δc_i can be translated into a nonlinear constrained optimization problem, which takes (27) as the objective function, and takes (26) as the constraints. An appropriate optimization algorithm can be adopted to solve this problem. For example, the genetic algorithm can be used in this nonlinear constrained optimization problem for its fine global search capability.

IV. SIMULATION AND EXPERIMENT

A. SIMULATION RESULTS

The simulation is implemented to illustrate the effectiveness of FCFCA in the process of the configuration control of MAF based on the 6 DOF kinematic and dynamic models of certain supersonic missile.

1) INITIAL CONDITIONS

The formation configuration control of MAF comprised of 6 missiles is cruising at 15000.0m height with a velocity of 3.0Ma in the safe corridor of 6000.0m according to the planned flight paths. In order to verify the efficiency of FCFCA more fully, the collision FC_{25} , of which the maneuvering space is the smallest, is designed. The configuration positions of v_2 and v_5 are designed to be exchanged at $t = 500.0s$. The initial conditions are shown in Table 1 and Fig. 4.

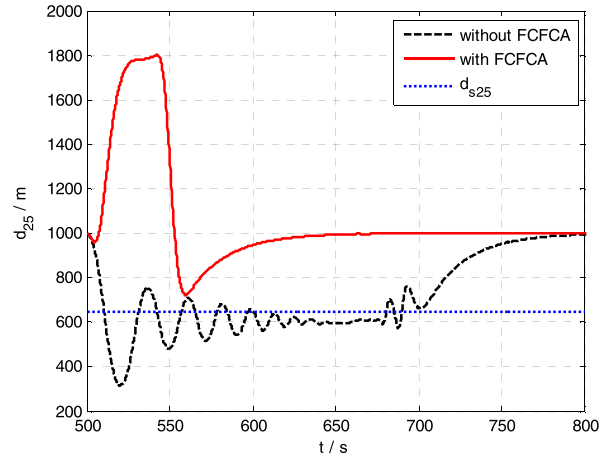
In Fig. 4, the white lines on both sides show the boundaries of safe corridor. The black line shows the flight path of MAF. E_i denotes the label of the missile node v_i . The blue and red lines, and the corresponding numbers are applied to describe the real-time distance d_{25} and d_{26} respectively.

Based on the characteristics of this type of missile, the parameters are as follows. $\forall i, j \in v, i \neq j, \sigma_i = 176.8m$, according to (1), $\sigma_{ij} = 250.0m$. Let $k_c = 1, d_{sij} = 650.0m, \mu_{ij} = 1000.0m$. Let $t_c = 0.02s, k_{qp} = 5.7$, according to (13), $m = 0.89 \in (0, 1)$ which explains the convergence of (10). The genetic algorithm with the group number set to 50 and the genetic algebra set to 20 is adopted to get the optimal transition vectors Δc_i .

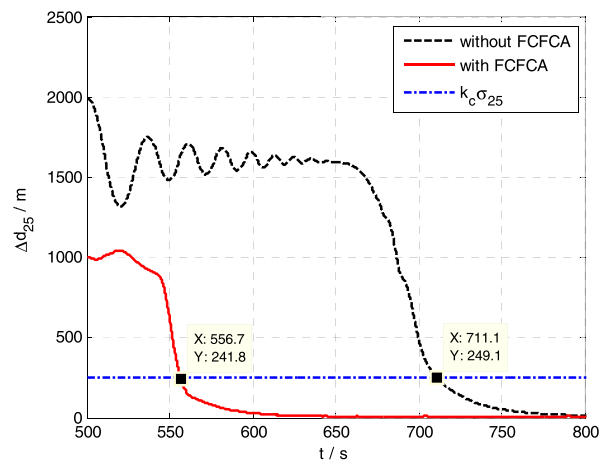
2) SIMULATION RESULTS WITHOUT FCFCA

The configuration control of MAF is controlled by the traditional formation configuration control algorithm without FCFCA. The process is shown in Fig. 5.

Since the directions of c_{25} and q_{25} are approximately reverse, v_2 and v_5 draw closely gradually (as shown in Fig. 5(a)). When $d_{25} \leq d_{s25}$, v_2 and v_5 draw separately gradually (as shown in Fig. 5(b)). The process repeats until the lateral distance increases gradually. Afterwards, v_2 gets the opportunity to go around v_5 (as shown in Fig. 5(c)–(d)), and then the configuration is formed gradually (as shown in Fig. 5(e)–(f)). In addition, a new collision FC_{26} ($d_{26} < d_{s26}$), i.e., the “chain effect”, occurs in the process of collision avoidance maneuvering between v_2 and v_5 (as shown in Fig. 5(d)).



(a)



(b)

FIGURE 8. Formation characteristics. (a) Distance between v_2 and v_5 . (b) Value of $\|c_{25} - q_{25}\|$.

3) SIMULATION RESULTS WITH FCFCA

The configuration control of MAF is controlled by optimized formation configuration control algorithm with FCFCA. The process is shown in Fig. 6.

The collisions $FC_{25}, FC_{32'}, FC_{62'}$ are forecast one after another, and the genetic algorithm is adopted to get $\Delta c_2 = (0.0, 1719.1), \Delta c_3 = (0.0, 1719.1), \Delta c_6 = (0.0, 1719.1)$. After the process of transition and restoration (as shown in Fig. 6(a)–(f)), MAF has formed the target configuration. In addition, during the process of the collision coordination, there is no other collision occurring, i.e., the “chain effect” is avoided.

4) COMPARISON RESULTS

The curves of velocity and lateral overload of v_2 and v_5 are shown in Fig. 7.

As shown in Fig. 7(a)–(d), when the configuration of MAF is controlled without FCFCA, v_2 and v_5 not only accelerate and decelerate frequently and drastically, but also make the

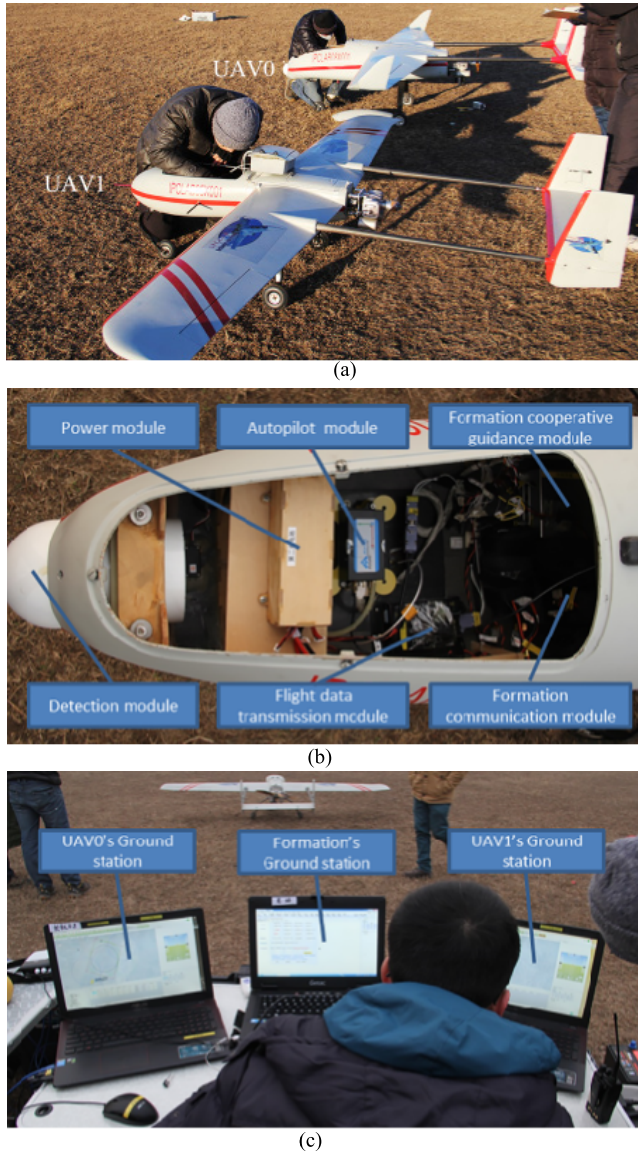


FIGURE 9. Multi-UAV formation flight experiment. (a) Two UAVs. (b) Module arrangement. (c) Ground station.

lateral maneuvering repeatedly. These are adverse to the flight stability of the supersonic missile in the high velocity cruise phase. Due to the introduction of FCFCA, the maneuvering above does not occur so that the whole process is relatively stable.

The formation characteristic curves are shown in Fig. 8.

Figure 8(a) shows the real time distance d_{25} curves of v_2 and v_5 . When the configuration is controlled without FCFCA, during the period of 511.2s ~ 689.5s, v_2 and v_5 switch between configuration forming and collision avoidance maneuvering repeatedly. Especially in the first collision avoidance maneuvering, $d_{25}|_{t=520.4} = 315.9m < d_{s25}$, which is adverse to the safety of MAF, although the collision avoidance algorithm reduces the distance in time. Due to

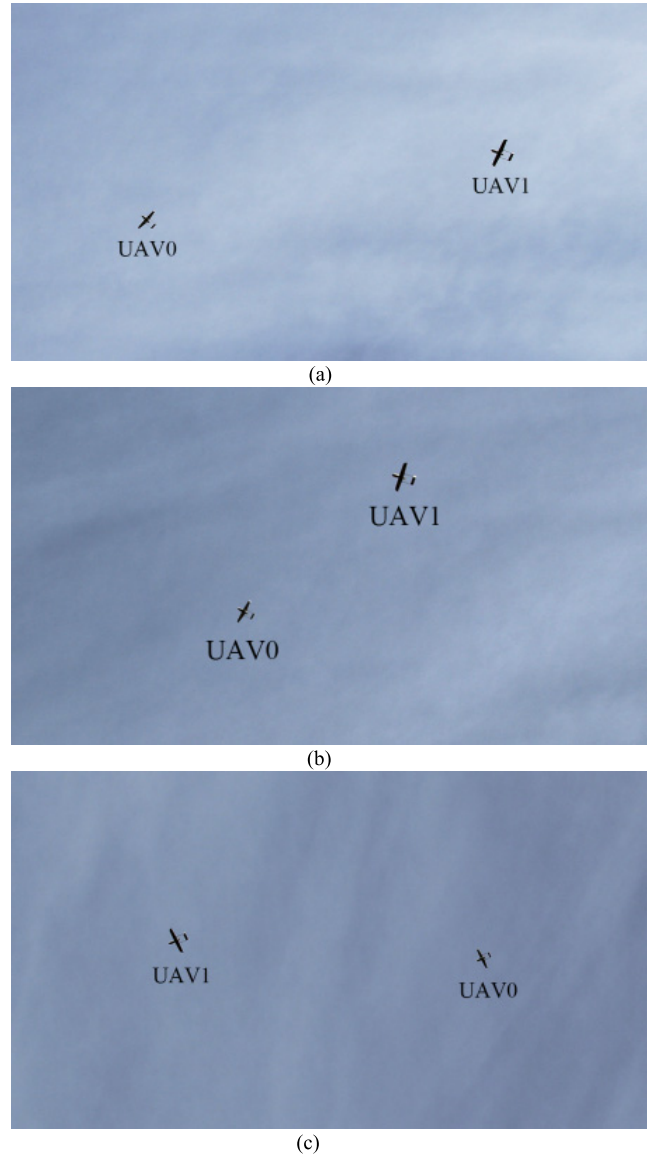


FIGURE 10. Multi-UAV formation control with FCFCA. (a) Before collision coordination. (b) During collision coordination. (c) Complete collision coordination.

the introduction of FCFCA, $d_{25} > d_{s25}$ is guaranteed, i.e., FCFCA avoids the collision between v_2 and v_5 successfully.

Figure 8(b) shows the modulus value curves $\Delta d_{25} = \|c_{25} - q_{25}\|$. When the configuration is controlled without FCFCA, $\Delta d_{25} \leq k_c \sigma_{ij}$ at $t \geq 711.1s$, which indicates that it takes $\Delta t_1 = 711.1 - 500.0 = 211.1s$ to finish the configuration control. When the configuration is controlled with FCFCA, $\Delta d_{25} \leq k_c \sigma_{ij}$ at $t \geq 556.7s$, which indicates that it takes $\Delta t_2 = 556.7 - 500.0 = 56.7s$ to finish the configuration control.

It can be found that the formation configuration control algorithm with FCFCA avoids formation collisions and the “chain effect” successfully, and guarantees the safety and stability of MAF. In the setting of this simulation, the formation configuration forming time is reduced

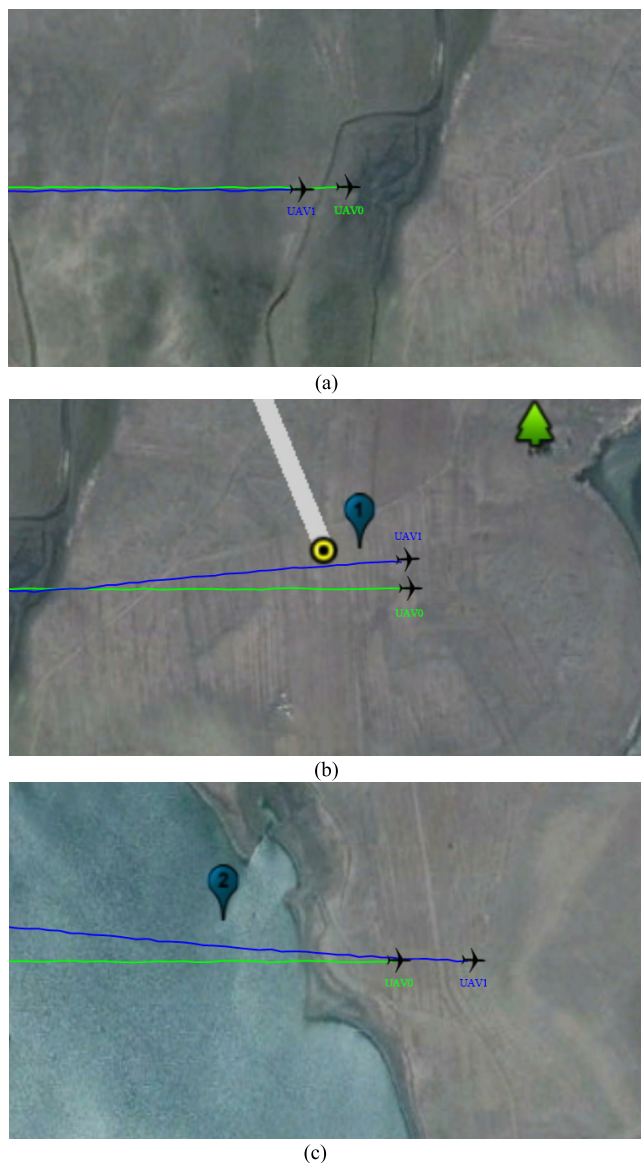


FIGURE 11. Multi-UAV formation recorded on the ground station. (a) Before collision coordination. (b) During collision coordination. (c) Complete collision coordination.

by 73.1% from 211.1s to 56.7s, so that efficiency of MAF is guaranteed.

B. EXPERIMENT RESULTS

In order to guide the engineering practice better, the multi-UAV (Unmanned Aerial Vehicle, UAV) outfield flight experiment is carried out to verify the effectiveness of FCFCA.

As shown in Fig. 9, the experiment is composed of two UAVs (UAV0 and UAV1) and three ground Stations. Each UAV is equipped with the power module, the autopilot module, the formation cooperative guidance module, the detection module, the flight data transmission module, the formation communication module and so on. The FCFCA proposed in this paper is in the formation cooperative guidance module.

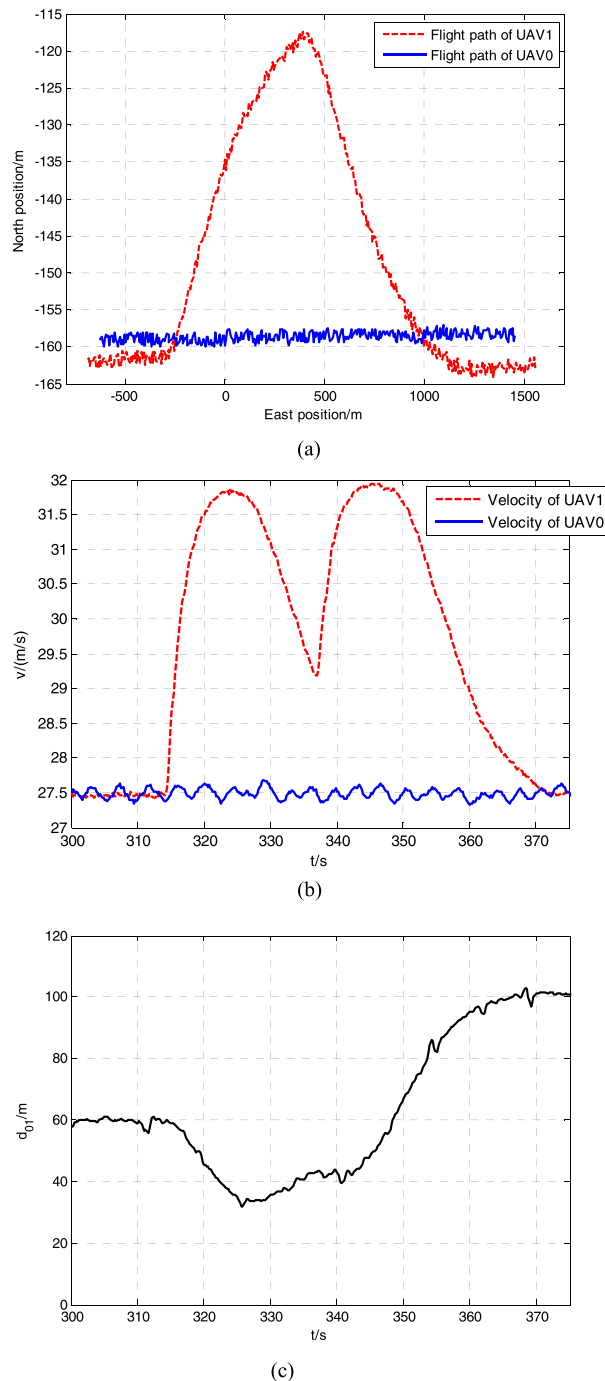


FIGURE 12. Flight data and figures of multi-UAV formation. (a) Flight path of UAV0 and UAV1. (b) Velocity of UAV0 and UAV1. (c) Distance between UAV0 and UAV1.

The ground stations are composed of two UAV’s ground stations (Substations) and one formation’s ground station (master station).

As shown in Fig. 10 and Fig. 11, at the beginning, UAV1 cruises 60.0m behind UAV0 at a height of 450.0m with a velocity of 27.5m/s. At a certain moment, the formation tends to reconstruct a new configuration, in which UAV1 is 100.0m in front of UAV0. FCFCA forecasts the collision FC_{01} in

the formation cooperative guidance module immediately. Then the optimal transition target configuration position $\Delta c_1 = (0.0, 50.0)$ of UAV1 is got to coordinate the collision. Therefore, UAV1 completes the reconstruction of formation through going around from the side of UAV0, so that the collision is avoided and the group cost of the formation is minimal.

The flight data and figures are shown as Fig. 12.

Fig. 12-(a) shows the whole flight path of UAV0 and UAV1 during the collision coordination. According to Fig. 12-(b), we can see that the first acceleration and deceleration of UAV1 are the process of forming transition target configuration position Δc_1 , and the second acceleration and deceleration are the process of forming the final target configuration of the formation. Moreover, the trough of the velocity figure indicates the time when the restoration command is made by FCFCA. The safe distance is set to be $d_{s01} = 26.0\text{m}$ based on the UAV's characteristic and the control accuracy, and from Fig. 12-(c) we can see the distance between UAV1 and UAV0 is always bigger than the safe distance, and the transition of the formation configuration is relatively stable. Therefore, the safety and stability of the formation are guaranteed with the introduction of FCFCA.

V. CONCLUSION

In this paper, a formation collision forecast and coordination algorithm has been proposed for missile autonomous formation. With the introduction of FCFCA, formation collisions and the "chain effect" are avoided effectively. Not only the formation configuration forming time is shortened, but also the safety and stability of formation configuration control are guaranteed.

However, there is still much to be researched further in this area. For example, the group cost of MAF is designed just based on distances. But in the practical application, the group cost may also include the constraints such as fuel consumption and radar reflection area. In the following research, these constraints should be considered.

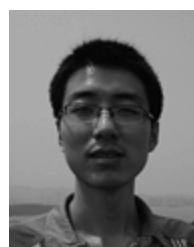
ACKNOWLEDGMENT

The authors would like to thank the editors and reviewers for their suggestions, which are of great value to the paper.

REFERENCES

- [1] S. T. Wu, "Flight control system of MAF," in *Cooperative Guidance & Control of Missile Autonomous Formation*, Beijing, China: National Defense Industry Press, 2015.
- [2] P. K. C. Wang, "Navigation strategies for multiple autonomous mobile robots moving in formation," *J. Robot. Syst.*, vol. 8, no. 2, pp. 177–195, 1991.
- [3] M. Anthony Lewis and K.-H. Tan, "High precision formation control of mobile robots using virtual structures," *Auton. Robots*, vol. 4, no. 4, pp. 378–403, 1997.
- [4] T. Balch and R. C. Arkin, "Behavior-based formation control for multi-robot teams," *IEEE Trans. Robot. Autom.*, vol. 14, no. 6, pp. 926–939, Jun. 1998.
- [5] M. Defoort, T. Floquet, A. Kokosy, and W. Perruquetti, "Sliding-mode formation control for cooperative autonomous mobile robots," *IEEE Trans. Ind. Electron.*, vol. 55, no. 11, pp. 3944–3953, Nov. 2008.

- [6] B. S. Park, J. B. Park, and Y. H. Choi, "Robust adaptive formation control and collision avoidance for electrically driven non-holonomic mobile robots," *IET Control Theory Appl.*, vol. 5, no. 3, pp. 514–522, Feb. 2011.
- [7] B. S. Park, J. B. Park, and Y. H. Choi, "Adaptive formation control of electrically driven nonholonomic mobile robots with limited information," *IEEE Trans. Syst., Man, Cybern. B, Cybern.*, vol. 41, no. 4, pp. 1061–1075, Aug. 2011.
- [8] Y. H. Chang, C. L. Chen, W. S. Chan, H. W. Lin, and C. W. Chang, "Fuzzy formation control and collision avoidance for multiagent systems," *Math. Probl. Eng.*, vol. 2013, no. 8, Jan. 2013, Art. no. 908180.
- [9] D. Shen, W. Sun, and Z. Sun, "Adaptive PID formation control of nonholonomic robots without leader's velocity information," *ISA Trans.*, vol. 53, no. 2, pp. 474–480, Mar. 2014.
- [10] S.-M. Lee and H. Myung, "Receding horizon particle swarm optimisation-based formation control with collision avoidance for non-holonomic mobile robots," *IET Control Theory Appl.*, vol. 9, no. 14, pp. 2075–2083, Sep. 2015.
- [11] B. J. Young, R. W. Beard, and J. M. Kelsey, "A control scheme for improving multi-vehicle formation maneuvers," in *Proc. Amer. Control Conf. Arlington*, Jun. 2001, pp. 704–709.
- [12] R. W. Beard, J. Lawton, and F. Y. Hadaegh, "A coordination architecture for spacecraft formation control," *IEEE Trans. Control Syst. Technol.*, vol. 9, no. 6, pp. 777–790, Nov. 2001.
- [13] W. Ren and R. W. Beard, "Formation feedback control for multiple spacecraft via virtual structures," *IEEE Proc. Control Theory Appl.*, vol. 151, no. 3, pp. 357–368, May 2004.
- [14] E. G. Hernandez-Martinez and E. A. Bricaire, "Non-collision conditions in multi-agent virtual leader-based formation control," *Int. J. Adv. Robot. Syst.*, vol. 9, no. 1, pp. 1–10, Oct. 2012.
- [15] P. Wang and B. C. Ding, "A synthesis approach of distributed model predictive control for homogeneous multi-agent system with collision avoidance," *Int. J. Control*, vol. 87, pp. 52–63, Jan. 2014.
- [16] P. Kostelnik, M. Samulka, and M. Janosik, "Scalable multi-robot formations using local sensing and communication," in *Proc. 3rd Int. Workshop Robot Motion Control*, Poznan, Poland, 2002, pp. 319–324.
- [17] X. Wang, V. Yadav, and S. N. Balakrishnan, "Cooperative UAV formation flying with obstacle/collision avoidance," *IEEE Trans. Control Syst. Technol.*, vol. 15, no. 4, pp. 672–679, Jul. 2007.
- [18] R. Falconi, L. Sabattini, C. Secchi, C. Fantuzzi, and C. Melchiorri, "Edge-weighted consensus-based formation control strategy with collision avoidance," *Robotica*, vol. 33, no. 2, pp. 332–347, Feb. 2015.
- [19] Y. Dai, K. S. Choi, and S. G. Lee, "Adaptive formation control and collision avoidance using a priority strategy for nonholonomic mobile robots," *Int. J. Adv. Robot. Syst.*, vol. 10, no. 2, pp. 323–330, Feb. 2013.
- [20] H. Fukushima, K. Kon, and F. Matsuno, "Model predictive formation control using branch-and-bound compatible with collision avoidance problems," *IEEE Trans. Robot.*, vol. 29, no. 5, pp. 1308–1317, Oct. 2013.
- [21] Y. Xia, X. Na, Z. Q. Sun, and J. Chen, "Formation control and collision avoidance for multi-agent systems based on position estimation," *Isa Trans.*, vol. 61, pp. 287–296, Mar. 2016.
- [22] C. W. Reynolds, "Flocks, herds, and schools: A distributed behavioral model," *Comput. Graph.*, vol. 21, no. 4, pp. 25–34, Jul. 1987.



YONGMING WEN was born in DaLian, China, in 1988. He is currently pursuing the Ph.D. degree at Beihang University, Beijing, China. He mainly studies the missile autonomous formation flight control system. In this article, he was mainly responsible for the design and simulation experiment of collision forecast and coordination algorithm.



SENTANG WU received the Ph.D. degree in dynamics, ballistics, and aircraft motion control systems from National Aviation University, Ukraine, in 1992.

He is currently a Professor of automation science and electrical engineering, and a Ph.D. Tutor at Beihang University, Beijing, China. He is also the Navy Missile expert with the National Defense Basic Research Institute and a member of the academic committee. His research interests include the theory and application of nonlinear stochastic systems, computer information processing and control, aircraft cooperative control, precision, and guidance.



WENLEI LIU is currently pursuing the Ph.D. degree at Beihang University, Beijing, China. His research interests include communication of missile autonomous formation. In this article, he contributed to the simulation to verify the effectiveness of FCFA.



JIA DENG is currently pursuing the Ph.D. degree at Beihang University, Beijing, China.

Her research interests include missile cooperative flight control and disc type vehicle. In this article, she contributed to the collision forecast and coordination algorithm.



XIONGJUN WU (M'12) is currently a Post-Doctoral with the 802nd Research Institute of Shanghai Academy of Space Flight Technology and the Eighth Academy of China Aerospace Science and Technology Corporation. His research interests include constraint control, robot control, visual servo and multi-agent control. He has authored about 80 papers and national defense science and technology reports, and holds East Asian patents.

Dr. Wu is a Senior Member of the Shanghai Aerospace Association.

...